Coordinating Active Distribution Networks with Multi-Microgrids: An ADMM-based Decentralized Adjustable Robust Operation Model

1st Junyi Zhai
State Grid (Suzhou) City & Energy Research Institute
Suzhou, China
Email: zhaijunyi@163.com

2nd Chenyixuan Ni
Department of Electronic, Electrical and Systems Engineering
University of Birmingham
Birmingham, United Kingdom
Email: CXN603@student.bham.ac.uk

3rd Philippe Nimmegeers
Department of Engineering Management, Environmental Economics (EnvEcon)
University of Antwerp
Antwerp, Belgium
Email: philippe.nimmegeers@uantwerpen.be

4th Yuning Jiang
Automatic Control Laboratory
École Polytechnique Fédérale de Lausanne
Lausanne, Switzerland
Email: yuning.jiang@epfl.ch

***Abstract*—This paper proposes a decentralized adjustable robust operation model achieving the coordinated operation between an active distribution network (ADN) and microgrids (MGs). Thanks to the autonomous characteristic and heterogeneity of the individual agents in ADNs with multi-MGs, we develop a tailored alternating direction method of multipliers (ADMM)-based fully decentralized framework. The linear decision rules are utilized to reformulate the microgrid two-stage adjustable robust operation problem as a computationally tractable solution such that the proposed adjustable robust extension of decentralized ADMM is capable of handling renewable energy uncertainties. The numerical results illustrate the effectiveness of the proposed model.**

***Index Terms*—Multi-microgrids, adjustable robust optimization, decentralized optimization**

NOMENCLATURE

Indices and Sets

$\mathcal{G}$	Subset of nodes with controllable DGs
$\mathcal{M}$	Set of MGs
$\mathcal{N}$	Set of nodes
$\mathcal{T}$	Set of periods
$\mathcal{U}$	Set of polyhedral uncertainty

Parameters

ϵ	Maximum deviation of voltage
η^C/η^D	Charging/discharging efficiency of ESS
κ	Uncertainty budget
$\overline{P}^{ex}/\overline{Q}^{ex}$	Exchanged active/reactive power limit between main grid and ADN
$\overline{P}_i^{DN}$	Exchanged active power limit between ADN and MG at node i
$\overline{P}_t^C/\overline{P}_t^D$	Maximum charging/discharging rate of ESS at time t
$\overline{P}_t^W/\overline{P}_t^P$	Predicted output of WT/PV at time t
$\overline{S}_i$	Transmission capacity limit from nodes i to $i+1$
$\underline{E}/\overline{E}$	Mimimum/maximum capacity of ESS
$\underline{V}_i/\overline{V}_i$	Mimimum/maximum voltage magnitude of node i
$a_i/b_i/c_i$	Fuel cost coefficients of controllable DG i
c^C/c^D	Charging/discharging cost of ESS
c_t^b/c_t^s	Buying/selling price from/to main grid at time t
$P_{i,t}^L$	Load demand of node i at time t
r_i/x_i	Line resistance/reactance between nodes i and $i+1$
R_i^D/R_i^U	Ramp-up/down limit of controllable DG i
$V_{0,t}$	Voltage of substation, normally 1 p.u.

Variables

E_t	Actual output of ESS at time t
P_t^b/P_t^s	Active power deficiency/surplus of ADN at time t
P_t^C/P_t^D	Charging/discharging power of ESS at time t
P_t^E	Actual output of ESS at time t
P_t^W/P_t^P	Actual output of WT/PV at time t
$P_t^{MG}/P_{i,t}^{DN}$	Active power injected to MG/flowing from ADN at node i in time t
$P_{1,t}/Q_{1,t}$	Exchanged active/reactive power between main grid and ADN at time t
$P_{i,t}/Q_{i,t}$	Active/reactive power from nodes i to $i+1$ at time t
$P_{i,t}^G/Q_{i,t}^G$	Active/reactive power of controllable DG at node i in time t
$V_{i,t}$	Voltage magnitude of node i at time t

Boldface lower case and upper case letters represent vectors and matrices, respectively.

I. INTRODUCTION

Restructuring power systems and the integration of renewable energy have transformed traditional distribution networks into active distribution networks (ADNs). The next step in this trend is to decentralize ADNs to microgrids (MGs), which are regarded as an effective way to improve the penetration rate of renewable energy and can provide powerful support for ADNs [1].

This work was supported in part from the Smart Grid Joint Foundation Program of National Natural Science Foundation of China and the State Grid Corporation of China (U1766212), in part from the Youth Program of Natural Science Foundation of Jiangsu Province (BK20210103), and in part from the Swiss National Science Foundation under the RISK project (Risk Aware Data Driven Demand Response, grant number 200021 175627) (Corresponding author: Yuning Jiang)

Recently, many studies have investigated the coordinated operation problem for ADN with multi-microgrids (MMG). In [2], a game theory based method that simulates the potential cooperative behaviors of MMG is proposed to achieve higher energy efficiency and operation economy. In [3], a two-stage collaborative operation model for a residential MMG is constructed while the interactive energy dispatch model between DN and residential MMG is addressed in [4]. However, these studies [2]–[4] all followed a centralized implementation. In practice, distribution system operator (DNO) and each microgrid operator (MGO) are respectively managed by different entities such that centralized optimization always leads to technical and political challenges. To this end, the decentralized framework becomes favorable as it does not require pooling all the local information as for a centralized operation.

The general distributed optimization algorithms can be classified into three types: 1) the augmented Lagrangian relaxation-based approaches such as the analytical target cascading (ATC) [5], alternating direction method of multipliers (ADMM) [6]–[8] and auxiliary problem principle (APP) [9]; 2) the Karush–Kuhn–Tucker conditions-based approaches such as the heterogeneous decomposition (HD) algorithm [10] and the optimality condition decomposition (OCD) algorithm [11]; and 3) the Benders' decomposition (BD) algorithm [12]. Among the augmented Lagrangian relaxation-based methods, ADMM has shown its superiority in convergence properties that has been adopted to the multi-area optimal power flow [6], energy market clearing [7], and energy Internet [8] problems.

Another challenge for the operation of multi-microgrid distribution networks is how to hedge uncertainties on renewable energy. Recently, stochastic optimization (SO) [13] and robust optimization (RO) [14]–[18] have attracted much attention. However, the exact probability distribution in SO is hard to obtain in practical applications. As a promising method, RO models characterize uncertain parameters through uncertainty sets and only need their constrained perturbations to find a solution optimized for the worst-case realization. Unlike the decomposition-based robust approach [14], [15], the linear decision rules (LDRs) [16]–[18] model can provide a slightly conservative yet single tractable solution to the robust adjustable formulation. Since the robust counterpart of the LDRs-based adjustable approach usually results in a tractable convex problem, the LDRs model is more suitable for decentralized optimization.

To achieve the synergistic yet independent operation of multiple entities, a fully decentralized operation framework is developed based on a tailored ADMM algorithm. This fully decentralized operation model can be solved in a parallel manner, achieving the synergistic yet independent operation of multiple entities. Then, the two-stage adjustable robust extension of decentralized ADMM capable of handling renewable energy uncertainties is proposed. The LDRs are utilized to solve the robust adjustable problems directly without decomposition, reducing the computational burden of every ADMM iteration and guaranteeing the convergence of ADMM.

II. Separable Formulation of Deterministic Operation Model

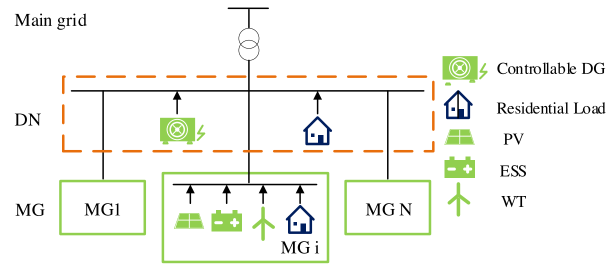

Fig. 1. Topology of distribution system with multi-microgrids

A typical topology of the multi-microgrids distribution system is shown in Fig.1. The MG organically combines the photovoltaic (PV), wind turbine (WT), and energy storage system (ESS) to meet local load demand.

A. Operation Problem of ADN

The optimization objective of ADN is to minimize the operation costs of controllable DGs as well as the power transaction costs including electricity purchasing costs or selling benefits from the main grid.

$$\min \sum_{t\in\mathcal{T}}\sum_{i\in\mathcal{G}}\left[a_i\left(P_{i,t}^G\right)^2+b_iP_{i,t}^G+c_i\right] + \sum_{t\in\mathcal{T}}\left(c_t^bP_t^b-c_t^sP_t^s\right) \tag{1a}$$

$$\text{s.t.}\quad P_{i+1,t}=P_{i,t}+P_{i+1,t}^G - P_{i+1,t}^L-P_{i+1,t}^{DN},\ i\in\mathcal{N},\ t\in\mathcal{T} \tag{1b}$$

$$Q_{i+1,t}=Q_{i,t}+Q_{i+1,t}^G-Q_{i+1,t}^L,\ i\in\mathcal{N},\ t\in\mathcal{T} \tag{1c}$$

$$V_{i+1,t}=V_{i,t}-\frac{r_iP_{i,t}+x_iQ_{i,t}}{V_{0,t}},\ i\in\mathcal{N},\ t\in\mathcal{T} \tag{1d}$$

$$P_{1,t}=P_t^b-P_t^s,\ P_t^b\geq 0,\ P_t^s\geq 0,\ t\in\mathcal{T} \tag{1e}$$

$$-\overline{P}^{ex}\leq P_{1,t}\leq\overline{P}^{ex},\ t\in\mathcal{T} \tag{1f}$$

$$-\overline{Q}^{ex}\leq Q_{1,t}\leq\overline{Q}^{ex},\ t\in\mathcal{T} \tag{1g}$$

$$P_{i,t}^2+Q_{i,t}^2\leq\overline{S}_i^2,\ i\in\mathcal{N},\ t\in\mathcal{T} \tag{1h}$$

$$1-\epsilon\leq V_{i,t}\leq 1+\epsilon,\ i\in\mathcal{N},\ t\in\mathcal{T} \tag{1i}$$

$$-\overline{P}_i^{DN}\leq P_{i,t}^{DN}\leq\overline{P}_i^{DN},\ i\in\mathcal{M},\ t\in\mathcal{T} \tag{1j}$$

$$\underline{P}_i^G\leq P_{i,t}^G\leq\overline{P}_i^G,\ i\in\mathcal{G},\ t\in\mathcal{T} \tag{1k}$$

$$-R_i^D\leq P_{i,t}^G-P_{i,t-1}^G\leq R_i^U,\ i\in\mathcal{G},\ t\in\mathcal{T} \tag{1l}$$

$$\underline{Q}_i^G\leq Q_{i,t}^G\leq\overline{Q}_i^G,\ i\in\mathcal{G},\ t\in\mathcal{T}. \tag{1m}$$

Constraints (1b)–(1d) are the linearized distribution load flow (Dist-Flow) equations. Constraints (1e)-(1g) represent the relationship between the power flow from the main grid to the ADN. Constraints (1h) denotes the branch capacity limit, which can be approximated by a number of linear constraints. Constraint (1i) ensures the voltage magnitude of each node is kept within the allowed maximum deviation from the nominal value. Constraint (1j) denotes the power flow limits transferred from ADN to MGs. Constraints (1k)-(1m) are the generation limits on controllable DGs.

B. Operation Problem of MG

The operation model of the k-th microgrid (omitting the subscript k to simplify the notation) is written as:

$$\min \sum_{t\in\mathcal{T}} \left(c^C P_t^C + c^D P_t^D\right) \tag{2a}$$

$$\text{s.t.} \quad P_t^W + P_t^P + P_t^D - P_t^C + P_t^{MG} = P_t^L,\ t\in\mathcal{T} \tag{2b}$$

$$-\overline{P}^{DN} \le P_t^{MG} \le \overline{P}^{DN},\ t\in\mathcal{T} \tag{2c}$$

$$0 \le P_t^W \le \overline{P}_t^W,\ t\in\mathcal{T} \tag{2d}$$

$$0 \le P_t^P \le \overline{P}_t^P,\ t\in\mathcal{T} \tag{2e}$$

$$0 \le P_t^C \le \overline{P}^C,\ t\in\mathcal{T} \tag{2f}$$

$$0 \le P_t^D \le \overline{P}^D,\ t\in\mathcal{T} \tag{2g}$$

$$E_t = E_{t-1} + \eta^C P_t^C - P_t^D/\eta^D,\ t\in\mathcal{T} \tag{2h}$$

$$\underline{E} \le E_t \le \overline{E},\ t\in\mathcal{T} \tag{2i}$$

$$E_0 = E_T. \tag{2j}$$

Constraint (2b) represents the power balance of MG while constraint (2c) denotes the power flow limits transferred from the MG to the ADN. Constraints (2d) and (2e) are the power production limit for WT and PV, respectively. Constraints (2f)-(2g) denote the charging/discharging rate limits of ESS. Constraint (2h) represents the energy balance of ESS. Constraint (2i) keeps the energy of ESS within its capacity limits. Constraint (2j) specifies the initial and final level of ESS.

C. Coupling of ADN and MGs

While implementing the decentralized optimization, it is necessary that the output power from the ADN should be equal to the input power to the MG.

$$P_{k,t}^{DN} = P_{k,t}^{MG},\ k\in\mathcal{M},\ t\in\mathcal{T}. \tag{3}$$

III. Compact LDRs-based Microgrid Adjustable Robust Operation Model

The adjustable robust model includes two stages, i.e., "here-and-now" and "wait-and-see". For the sake of presentation, we write the deterministic operation model of each MG into the following compact epigraph form:

$$\min_{\boldsymbol{x},\boldsymbol{y}} \ \Phi(\boldsymbol{x},\boldsymbol{y}) \tag{4a}$$

$$\text{s.t.} \quad \boldsymbol{A}\cdot\boldsymbol{x} + \boldsymbol{B}\cdot\boldsymbol{y} + \boldsymbol{C}\cdot\hat{\boldsymbol{\xi}} + \boldsymbol{e} = 0, \tag{4b}$$

$$\boldsymbol{D}\cdot\boldsymbol{x} + \boldsymbol{E}\cdot\boldsymbol{y} + \boldsymbol{F}\cdot\hat{\boldsymbol{\xi}} + \boldsymbol{f} \le 0 \tag{4c}$$

with coefficient matrices $\boldsymbol{A}$, $\boldsymbol{B}$, $\boldsymbol{C}$, $\boldsymbol{D}$, $\boldsymbol{E}$, and $\boldsymbol{F}$ in appropriate dimension, $\boldsymbol{e}$, $\boldsymbol{f}$ denote the requirement vectors, $\boldsymbol{x}$ denotes the "here-and-now" variables made before the realization of uncertainty, variables $\boldsymbol{y}$ can take "wait-and-see" recourse decisions, function $\Phi(\cdot,\cdot)$ denotes the compact linear objective, $\hat{\boldsymbol{\xi}}$ denotes a forecast value of the uncertainty of renewable energy denoted by vector $\boldsymbol{\xi}$.

In this paper, the uncertain parameter $\boldsymbol{\xi}$ is restricted by being in a polyhedral uncertainty set given by

$$\mathcal{U} = \{\boldsymbol{\xi} \ge 0,\ \boldsymbol{K}\cdot\boldsymbol{\xi} - \boldsymbol{g} \le 0\}. \tag{5}$$

The robustness level can be controlled using a parameter denominated as the budget of uncertainty. The robust form of (4c) can be thus, written as the following semi-infinite form:

$$\forall \boldsymbol{\xi}\in\mathcal{U},\quad \boldsymbol{D}\cdot\boldsymbol{x} + \boldsymbol{E}\cdot\boldsymbol{y} + \boldsymbol{F}\cdot\boldsymbol{\xi} + \boldsymbol{f} \le 0, \tag{6}$$

The decision variable $\boldsymbol{y}$ is replaced by an LDR including two parts,

$$\boldsymbol{y} = \boldsymbol{y}^{\mathrm{N}} + \boldsymbol{y}^{\mathrm{A}}\cdot\boldsymbol{\xi}, \tag{7}$$

where non-adjustable variable $\boldsymbol{y}^{\mathrm{N}}$ is the "here-and-now" part made before the realization of uncertainty while adjustable variable $\boldsymbol{y}^{\mathrm{A}}$ is the "wait-and-see" part made after the uncertain parameters are revealed.

Thus, (6) can be further rewritten as

$$\forall \boldsymbol{\xi}\in\mathcal{U},\quad \boldsymbol{D}\cdot\boldsymbol{x} + \boldsymbol{E}\cdot\left(\boldsymbol{y}^{\mathrm{N}} + \boldsymbol{y}^{\mathrm{A}}\cdot\boldsymbol{\xi}\right) + \boldsymbol{F}\cdot\boldsymbol{\xi} + \boldsymbol{f} \le 0. \tag{8}$$

The constraint (8) is feasible for any realization of the uncertain parameters if it is feasible for the worst-case realization of the uncertain parameters such that (8) is equivalent to

$$\max_{\boldsymbol{\xi}\in\mathcal{U}} \left\{\boldsymbol{E}\cdot\left(\boldsymbol{y}^{\mathrm{N}} + \boldsymbol{y}^{\mathrm{A}}\cdot\boldsymbol{\xi}\right) + \boldsymbol{F}\cdot\boldsymbol{\xi}\right\} + \boldsymbol{D}\cdot\boldsymbol{x} + \boldsymbol{f} \le 0. \tag{9}$$

The worst-case constraint (9) can be further simplified by using duality theory [19] to eliminate the max operator such that the robust form of (4) is given by

$$\min_{\boldsymbol{x},\boldsymbol{y}^{\mathrm{N}},\boldsymbol{y}^{\mathrm{A}},\boldsymbol{\Lambda},\boldsymbol{\Pi}} \ \overline{\Phi}\left(\boldsymbol{x},\boldsymbol{y}^{\mathrm{N}},\boldsymbol{y}^{\mathrm{A}},\boldsymbol{\Lambda}\right) \tag{10a}$$

$$\text{s.t.} \quad \boldsymbol{A}\cdot\boldsymbol{y} + \boldsymbol{B}\cdot\boldsymbol{y}^{\mathrm{N}} + \boldsymbol{C}\cdot\hat{\boldsymbol{\xi}} + \boldsymbol{e} = 0 \tag{10b}$$

$$\boldsymbol{D}\cdot\boldsymbol{y} + \boldsymbol{E}\cdot\boldsymbol{y}^{\mathrm{N}} + \boldsymbol{\Pi}^{\top}\cdot\boldsymbol{g} + \boldsymbol{f} \le 0 \tag{10c}$$

$$\boldsymbol{\Pi}^{\top}\cdot\boldsymbol{K} \ge \boldsymbol{E}\cdot\boldsymbol{y}^{\mathrm{A}} + \boldsymbol{F} \tag{10d}$$

$$\boldsymbol{\Lambda},\ \boldsymbol{\Pi} \ge 0 \tag{10e}$$

with associated dual variable $\boldsymbol{\Lambda}$ and $\boldsymbol{\Pi}$. Here, the reformulation of the worst-case objective is the same as the reformulation of constraints (9) by using the duality theory such that $\overline{\Phi}$ is also linear [20].

IV. Fully Decentralized Adjustable Robust Operation Framework

We stack by $\boldsymbol{\chi}_a$ the local decision variables such that the adjustable robust operation model for ADN with MMG can be summarized into an affine-coupled separable form

$$\min_{\boldsymbol{x}} \ \sum_{a\in\mathcal{R}} \Psi_a(\boldsymbol{\chi}_a) \tag{11a}$$

$$\text{s.t.} \quad \boldsymbol{\Gamma}_{a,b}\boldsymbol{\chi}_a = \boldsymbol{\Gamma}_{b,a}\boldsymbol{\chi}_b\ ,\ (a,b)\in\mathcal{V} \tag{11b}$$

$$\boldsymbol{\chi}_{\boldsymbol{a}} \in \mathcal{X}_a\ ,\ a\in\mathcal{R} \tag{11c}$$

with local objective Ψ_a, and local constraint set $\mathcal{X}_a$, $a\in\mathcal{R}$ collects all decoupled constraints and their associated robust tractable reformulation introduced in Section II and III for the ADN and each MMG. Here, $\mathcal{R}$ denotes the index of local systems including the ADN and MMGs, the coupled affine equality constraint (11b) summarizes constraints (3) for all $(a,b) \in \mathcal{V}$, where $\mathcal{V} \subseteq \mathcal{R} \times \mathcal{R}$ denotes the pair of neighboring local systems.

In order to solve (11) using ADMM in a fully decentralized manner, we introduce consensus variables $\boldsymbol{\zeta}$ with the following affine equalities

$$\boldsymbol{\Gamma}_{a,b}\boldsymbol{\chi}_a = \boldsymbol{\zeta}_{a,b}\ ,\ \boldsymbol{\Gamma}_{b,a}\boldsymbol{\chi}_b = \boldsymbol{\zeta}_{a,b}\ ,\ (a,b) \in \mathcal{V} \tag{12}$$

where $\boldsymbol{\zeta}_{a,b}$ includes the elements of $\boldsymbol{\zeta}$ w.r.t. the coupling between local system a and b. Then, we stack all local consensus variables into the compact form

$$\boldsymbol{\Gamma}_a\boldsymbol{\chi}_a = \boldsymbol{\zeta}_a\ ,\ a \in \mathcal{R}\ . \tag{13}$$

In a result, the augmented Lagrangian is written as

$$L(\boldsymbol{\chi},\boldsymbol{\zeta},\boldsymbol{\lambda}) := \sum_{a\in\mathcal{R}} \left\{ \Psi_a(\boldsymbol{\chi}_a) + \boldsymbol{\lambda}_a^\top(\boldsymbol{\Gamma}_a\boldsymbol{\chi}_a - \boldsymbol{\zeta}_a) + \frac{\rho_a}{2}\|\boldsymbol{\Gamma}_a\boldsymbol{\chi}_a - \boldsymbol{\zeta}_a\|_2^2 \right\}\ ,$$

where $\boldsymbol{\lambda}_a$ denotes the Lagrangian multipliers of (13). The synchronous ADMM iteration is thus, given by

$$\begin{aligned}
\boldsymbol{\chi}_a^{\ell+1} &= \underset{\boldsymbol{\chi}_a\in\mathcal{X}_a}{\text{argmin}}\ \Psi_a(\boldsymbol{\chi}_a) + {\boldsymbol{\lambda}_a^{\ell}}^\top\left(\boldsymbol{\Gamma}_a\boldsymbol{\chi}_a - \boldsymbol{\zeta}_a^\ell\right) && \text{(14a)}\\
&\qquad + \frac{\rho_a}{2}\left\|\boldsymbol{\Gamma}_a\boldsymbol{x}_a - \boldsymbol{\zeta}_a^\ell\right\|_2^2\ ,\ a \in \mathcal{R}\\
\boldsymbol{\lambda}_a^{\ell+1} &= \boldsymbol{\lambda}_a^\ell + \rho_a(\boldsymbol{\Gamma}_a\boldsymbol{\chi}_a^{\ell+1} - \boldsymbol{\zeta}_a^\ell)\ ,\ a \in \mathcal{R} && \text{(14b)}\\
\boldsymbol{\zeta}_{a,b}^{\ell+1} &= \underset{\boldsymbol{\zeta}_{a,b}}{\text{argmin}}\ (\boldsymbol{\Gamma}_{a,b}\boldsymbol{\chi}_a^{\ell+1} - \boldsymbol{\zeta}_{a,b})^\top\boldsymbol{\lambda}_{a,b}^{\ell+1} && \text{(14c)}\\
&\quad + \frac{\rho_a}{2}\left\|\boldsymbol{\Gamma}_{a,b}\boldsymbol{\chi}_a^{\ell+1} - \boldsymbol{\zeta}_{a,b}\right\|_2^2 + (\boldsymbol{\Gamma}_{b,a}\boldsymbol{x}_b^{\ell+1} - \boldsymbol{\zeta}_{a,b})^\top\boldsymbol{\lambda}_{b,a}^{\ell+1}\\
&\quad + \frac{\rho_b}{2}\left\|\boldsymbol{\Gamma}_{b,a}\boldsymbol{\chi}_b^{\ell+1} - \boldsymbol{\zeta}_{a,b}\right\|_2^2\\
&= \frac{\boldsymbol{\Gamma}_{b,a}\boldsymbol{\chi}_b^{\ell+1} + \boldsymbol{\Gamma}_{a,b}\boldsymbol{\chi}_a^{\ell+1} - \boldsymbol{\lambda}_{a,b}^{\ell+1} - \boldsymbol{\lambda}_{b,a}^{\ell+1}}{\rho_a + \rho_b}, (a,b) \in \mathcal{V}.
\end{aligned}$$

Here, ℓ denotes a global iteration counter. The local primal update (14a) and dual update (14b) can be employed in parallel while the consensus update (14c) can be proceed either by local system a or b.

V. Numerical Results

To evaluate the algorithm, numerical simulations were performed on the modified IEEE-69 bus system [21] with four MGs located at nodes 27, 46, 50, and 65. The day-ahead electricity market price, the operating characteristics of controllable DGs and ESSs, the day-ahead output of PVs and WTs, and other detailed parameters can be found at [22]. The initial values of coupling variables and multipliers are all set to 0. To simplify the analysis, the uncertainty budgets of each MG are assumed the same. The case study is implemented in Matlab R2016a on an Intel Core i7-8700, 3.2 GHz, 16 GB RAM computer, solved by `Gurobi 9.0`.

A. Comparison of Different Variation Ranges

Three different robust cases with different variation ranges for PVs and WTs are considered here: Case 1 (10%), Case 2 (20%), and Case 3 (30%). The following observations can be obtained:

1) For budget $\kappa = 0$, the operation costs of all cases are identical. This is because when the uncertainty budget is zero, no uncertain parameters can deviate from their forecasts. Thus, budget $\kappa = 0$ leads to the deterministic model, which yields the same results for different variation ranges.

2) For a specific variation range, by increasing budget κ, the solution becomes more robust at the expense of higher operation costs. As shown in Table I, we can see that as budget κ increases, the total operation costs monotonically increase until $\kappa = 0.25$. In other words, $\kappa = 0.25$ is the point with the maximum robustness level in which all uncertain parameters have adopted their worst-case realizations.

3) For a specific value of uncertainty budget, the operation costs increase by increasing the variation range. This is because a greater variation range allows the uncertain renewable energies to deviate more from their forecasts, which leads to a worse worst-case realization.

4) The computational burden of the proposed LDR-based two-stage adjustable RO model is very low, which facilitates its application to the real-life applications.

TABLE I
COMPARISON OF DIFFERENT UNCERTAINTY BUDGETS

κ	Total operation cost (\$)			Average time (s)
	Case 1	Case 2	Case 3	
0	1980.41	1980.41	1980.41	3.62
0.05	2046.82	2121.59	2200.92	4.71
0.1	2068.42	2171.38	2284.02	4.66
0.15	2075.24	2185.97	2307.81	4.70
0.2	2080.97	2197.69	2325.86	4.68
0.25	2085.74	2207.26	2340.33	4.54

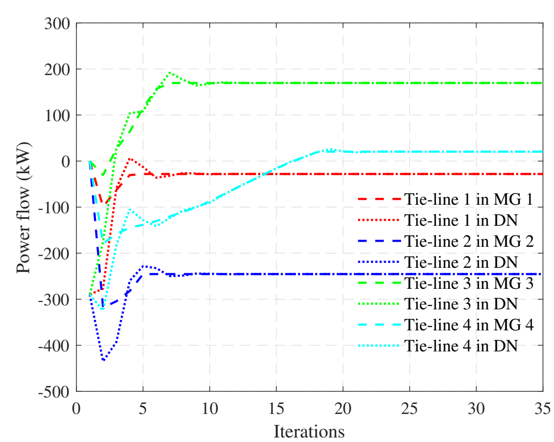

Fig. 2. Convergence of tie-line power flow

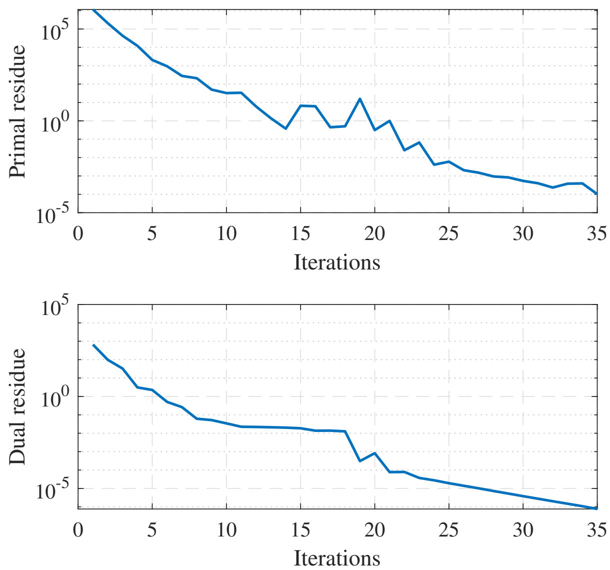

Fig. 3. Convergence of maximum primal and dual residue

B. Convergence Performance and Solution Quality

Taking hour 4 in Case 2 as an example and assuming that the uncertainty budgets of MGs are all 0.2, the iteration process of the ADMM algorithm on the tie-line power is depicted in Fig. 2. The convergence of the maximum primal and dual residue over the scheduling cycle is shown in Fig. 3. The tailored ADMM algorithm converges after 35 iterations with all the primal and dual residues smaller than the thresholds. The tailored ADMM-based decentralized optimization scheme is compared with the centralized scheme to demonstrate its solution quality, summarized in Table II. The converged operation cost found by the decentralized ADMM algorithm is nearly the same as that identified by the centralized method. The solution gap is 0.0005%, which is fairly small.

TABLE II
COMPARISON OF DIFFERENT ALGORITHMS

Algorithm	Iterations	Total operation cost ($)	Solution gap
Centralized	-	2197.69	-
Decentralized	35	2197.70	0.0005%

VI. CONCLUSIONS

This paper proposes the fully decentralized adjustable robust operation model for active distribution system with multi-microgrids. The decomposed microgrid operation problem is formulated as a LDRs-based two-stage adjustable robust model, which models both "here-and-now" and "wait-and-see" decision variables and provides robustness against renewable energy uncertainties. The proposed fully decentralized operation framework can preserve the information privacy and the decision independency of both distribution network and microgrids.

REFERENCES

[1] P. Wu, W. Huang, N. Tai, and S. Liang, "A novel design of architecture and control for multiple microgrids with hybrid ac/dc connection," *Applied Energy*, vol. 210, pp. 1002 – 1016, 2018.

[2] Y. Du, Z. Wang, G. Liu, X. Chen, H. Yuan, Y. Wei, and F. Li, "A cooperative game approach for coordinating multi-microgrid operation within distribution systems," *Applied Energy*, vol. 222, pp. 383–395, 2018.

[3] B. Zhang, Q. Li, L. Wang, and W. Feng, "Robust optimization for energy transactions in multi-microgrids under uncertainty," *Applied Energy*, vol. 217, pp. 346–360, 2018.

[4] T. Sattarpour, S. Golshannavaz, D. Nazarpour, and P. Siano, "A multi-stage linearized interactive operation model of smart distribution grid with residential microgrids," *International Journal of Electrical Power Energy Systems*, vol. 108, pp. 456–471, 2019.

[5] A. Kargarian, Y. Fu, and Z. Li, "Distributed security-constrained unit commitment for large-scale power systems," *IEEE Transactions on Power Systems*, vol. 30, no. 4, pp. 1925–1936, 2015.

[6] V. Rostampour, O. t. Haar, and T. Keviczky, "Distributed stochastic reserve scheduling in ac power systems with uncertain generation," *IEEE Transactions on Power Systems*, vol. 34, no. 2, pp. 1005–1020, 2019.

[7] Y. Zhang and G. B. Giannakis, "Distributed stochastic market clearing with high-penetration wind power," *IEEE Transactions on Power Systems*, vol. 31, no. 2, pp. 895–906, 2016.

[8] H. Zhang, Y. Li, D. W. Gao, and J. Zhou, "Distributed optimal energy management for energy internet," *IEEE Transactions on Industrial Informatics*, vol. 13, no. 6, pp. 3081–3097, 2017.

[9] C. Liu, J. Wang, Y. Fu, and V. Koritarov, "Multi-area optimal power flow with changeable transmission topology," *IET Generation, Transmission Distribution*, vol. 8, no. 6, pp. 1082–1089, 2014.

[10] Z. Li, Q. Guo, H. Sun, and J. Wang, "Coordinated economic dispatch of coupled transmission and distribution systems using heterogeneous decomposition," *IEEE Transactions on Power Systems*, vol. 31, no. 6, pp. 4817–4830, 2016.

[11] A. G. Bakirtzis and P. N. Biskas, "A decentralized solution to the dc-opf of interconnected power systems," *IEEE Transactions on Power Systems*, vol. 18, no. 3, pp. 1007–1013, 2003.

[12] C. Lin, W. Wu, B. Zhang, and Y. Sun, "Decentralized solution for combined heat and power dispatch through benders decomposition," *IEEE Transactions on Sustainable Energy*, vol. 8, no. 4, pp. 1361–1372, 2017.

[13] A. R. Malekpour and A. Pahwa, "Stochastic networked microgrid energy management with correlated wind generators," *IEEE Transactions on Power Systems*, vol. 32, no. 5, pp. 3681–3693, 2017.

[14] Z. Li, W. Wu, B. Zeng, M. Shahidehpour, and B. Zhang, "Decentralized contingency-constrained tie-line scheduling for multi-area power grids," *IEEE Transactions on Power Systems*, vol. 32, no. 1, pp. 354–367, 2017.

[15] C. He, L. Wu, T. Liu, and M. Shahidehpour, "Robust co-optimization scheduling of electricity and natural gas systems via admm," *IEEE Transactions on Sustainable Energy*, vol. 8, no. 2, pp. 658–670, 2017.

[16] A. Attarha, P. Scott, and S. Thiébaux, "Affinely adjustable robust admm for residential der coordination in distribution networks," *IEEE Transactions on Smart Grid*, vol. 11, no. 2, pp. 1620–1629, 2020.

[17] S. Dehghan, N. Amjady, and A. J. Conejo, "Adaptive robust transmission expansion planning using linear decision rules," *IEEE Transactions on Power Systems*, vol. 32, no. 5, pp. 4024–4034, 2017.

[18] R. A. Jabr, "Linear decision rules for control of reactive power by distributed photovoltaic generators," *IEEE Transactions on Power Systems*, vol. 33, no. 2, pp. 2165–2174, 2018.

[19] S. Boyd, S. P. Boyd, and L. Vandenberghe, *Convex optimization*. Cambridge university press, 2004.

[20] P. Xiong and P. Jirutitijaroen, "A linear decision rule approach for robust unit commitment considering wind power generation," in *2014 Power Systems Computation Conference*, pp. 1–7, IEEE, 2014.

[21] J. S. Savier and D. Das, "Impact of network reconfiguration on loss allocation of radial distribution systems," *IEEE Transactions on Power Delivery*, vol. 22, no. 4, pp. 2473–2480, 2007.

[22] https://github.com/JunyiZhai1990/ADN-with-MMG.